

New Critical Behavior in the Dense Two-Dimensional Classical Coulomb Gas

Jong-Rim Lee and S. Teitel

Department of Physics and Astronomy, University of Rochester, Rochester, New York 14627

(Received 29 December 1989)

We carry out Monte Carlo simulations of the two-dimensional classical neutral Coulomb gas of integer charges on a square lattice, as a function of temperature and chemical potential, and find new critical behavior. At low temperature, as density increases, the system has a first-order transition to an ordered-charge lattice. As temperature increases, this dense phase has a Kosterlitz-Thouless transition followed by an Ising transition. The first-order line joins the line of Ising transitions at a new tricritical point.

PACS numbers: 05.50.+q, 64.60.-i

The two-dimensional classical neutral Coulomb gas (CG) of integer charges has been the subject of much theoretical research.¹ Via the mapping to the 2D XY model,² the CG has served as a model for the behavior of vortices in superconducting and superfluid films.³ In the low-density limit, the CG has a Kosterlitz-Thouless (KT) transition.⁴ As the temperature T is increased, the inverse dielectric function $\epsilon^{-1}(T)$ has a universal discontinuous jump to zero.⁵ At higher densities, however, there have been suggestions that the transition may be more complicated. Several workers⁶ have introduced modified XY models and found evidence for a first-order transition. More recently, Minnhagen⁷ has studied higher-order corrections to the KT scaling equations in the continuum CG, finding nonuniversal jumps in ϵ^{-1} at high densities. This has been associated with a first-order liquid-gas transition in the charge density.⁸ A direct simulation of the CG in the dense limit is therefore of great interest. Uniformly frustrated XY models, which describe Josephson arrays in a magnetic field, can be described in terms of a dense Coulomb gas of fractional charges.⁹ Non-KT features of the transition have been found in these systems, due to the domainlike excitations which become possible in these dense systems.⁹⁻¹¹ Study of the dense-integer CG may thus improve our understanding of these uniformly frustrated XY models as well.

We present here the first direct Monte Carlo simulations of the 2D neutral-integer CG where the chemical potential is directly varied to study the dense limit. We find new critical behavior, including a new tricritical point. The Hamiltonian we study is

$$\mathcal{H} = \frac{1}{2} \sum_{i,j} q_i V'(\mathbf{r}_i - \mathbf{r}_j) q_j - u \sum_i q_i^2 + \sum_i (q_i^4 - q_i^2). \quad (1)$$

The first term above is the ordinary Coulomb gas: The sum is over all pairs of sites of a square lattice; $V'(\mathbf{r}) \equiv V(\mathbf{r}) - V(0)$, where $V(\mathbf{r})$ solves $D_{ij}V(\mathbf{r}_i - \mathbf{r}_j) = -2\pi\delta_{ij}$ with D_{ij} the lattice Laplacian, is the two-dimensional Coulomb potential with singularity removed; $q_i = 0, \pm 1, \pm 2, \dots$ is the integer charge at site i ; and neutrality $\sum_i q_i = 0$ is imposed. The second term controls the chemical potential for charges; increasing u

increases the average charge density. The third term helps suppress charges with $|q_i| > 1$ and is necessary to stabilize the system in the very dense limit.

Our results are summarized by the u - T phase diagram shown in Fig. 1. At small u and T , in the insulating phase \mathcal{A} , the ground state is the vacuum and charges exist in bound neutral pairs. As T increases from within \mathcal{A} , there is a KT transition (dashed line) to a conducting phase \mathcal{B} determined by the vanishing of ϵ^{-1} . At small T within \mathcal{A} , as u increases (increasing density), there is a first-order transition (thick solid line) to an insulating phase \mathcal{D} . In \mathcal{D} , the ground state is an ordered-checkerboard lattice of $+1, -1$ charges, which is doubly degenerate and characterized by an Ising-like order parameter M (analogous to the staggered magnetization of an Ising antiferromagnet). As T increases within \mathcal{D} , there is first a KT transition (dashed line) to a conducting phase \mathcal{E} , measured by the vanishing of ϵ^{-1} . This is followed by a transition to phase \mathcal{B} , measured by the

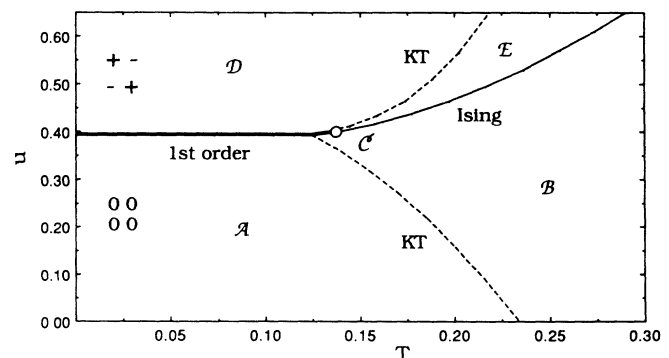


FIG. 1. Phase diagram for the classical neutral-integer-charge 2D Coulomb gas, as a function of temperature T and parameter u . Increasing u increases the average charge density. Dashed lines are Kosterlitz-Thouless transitions where the dielectric function ϵ diverges. The thick solid line is a first-order transition to a charge lattice ground state. The thin solid line is an Ising-like second-order transition at which the charge lattice melts. \mathcal{C} is a tricritical point where the Ising and first-order lines meet. The KT lines meet the first-order line at a temperature below \mathcal{C} .

vanishing of the Ising order parameter M (thin solid line). This combination of XY and Ising transitions is reminiscent of behavior in the fully frustrated XY model.⁹⁻¹¹ The first-order line and the Ising line meet at a new tricritical point \mathcal{C} . The KT lines meet the first-order line at a temperature below the critical point \mathcal{C} . At both KT lines, we find no strong evidence for nonuniversal jumps in ϵ^{-1} .

The first-order line is easily explained. Taking the Fourier transform of the first two terms in the Hamiltonian (1) gives $\mathcal{H} = \sum_k (\frac{1}{2} V_k - u) q_k q_{-k}$. When u becomes greater than $\min_k (\frac{1}{2} V_k)$, the system will order in a state with nonzero average q_k . As $\min(V_k) = \pi/4$ at $\mathbf{k} = \pi\hat{x} + \pi\hat{y}$, there is a discontinuous change in ground state to the checkerboard lattice at $u_c = \pi/8$. The third term in \mathcal{H} , Eq. (1), stabilizes the lattice at unit charges.

The rest of the phase diagram we map out using Monte Carlo simulations on square lattices with $N = L^2$ sites, and periodic boundary conditions. $V(\mathbf{r})$ is computed exactly by Fourier transform.¹⁰ At each step of the simulation, a nearest-neighbor pair (i, j) is selected at random; q_i is increased by one, and q_j decreased by one. This excitation is then either accepted or rejected according to the standard Metropolis algorithm.

The line of Ising transitions in the dense phase is given by observing a temperature at which the specific heat C scales logarithmically with size (from $L=4$ to 16) at values $u=0.45, 0.5$, and 0.6 . The Ising order parameter $M \equiv (1/N) \sum_i q_i (-1)^{x_i + y_i}$ is also observed to vanish on this line. At $u=0.4$, however, where the Ising line meets the first-order line, distinctly non-Ising scaling is observed. As the Ising and first-order lines appear to meet tangentially, we assume \mathcal{C} to be a tricritical point rather than a critical end point.

Scaling of the free energy $f \equiv -(1/N) \ln Z$ near a tricritical point is given by¹²

$$f(g_1, g_2, h, L) \sim L^{-d} f(g_1 L^{y_1}, g_2 L^{y_2}, h L^{y_h}, 1), \quad (2)$$

where the scaling fields $g_1(T, u)$ and $g_2(T, u)$ give the most, and next most, relevant directions in the u - T phase space ($y_1 > y_2 > 0$); $g_{1c} = g_{2c} = 0$, and h is a field which couples to the order parameter M . Assuming that the T direction at \mathcal{C} has a nonzero projection onto g_1 , we have for the leading finite-size behavior of the specific heat

$$C(L) = \frac{1}{NT^2} (\langle \mathcal{H}^2 \rangle - \langle \mathcal{H} \rangle^2) \\ = -\frac{1}{T^2} \frac{\partial^2 f}{\partial K^2} \sim L^{2y_1 - d}, \quad (3)$$

$$-f_{ee} = \frac{T\chi_q s^2 + (2/NT) (\langle \mathcal{H} \sum_i q_i^2 \rangle - \langle \mathcal{H} - T \rangle \langle \sum_i q_i^2 \rangle) * s + C}{T^2(1+s^2)}, \quad (5)$$

where $s \equiv du/dT$ is the slope of the unit vector \hat{e} . For any direction with $\hat{e} \cdot \hat{g}_1 \neq 0$, we expect the scaling $L^{2y_1 - d}$. For $\hat{e} \cdot \hat{g}_1 = 0$, however, the scaling $L^{2y_2 - d}$ is expected. By varying the direction \hat{e} we find the most relevant direction g_1 as that giving the greatest growth in f_{ee} with L ; we find the direction g_2 as that of least growth in f_{ee} with L . In Fig. 3 we

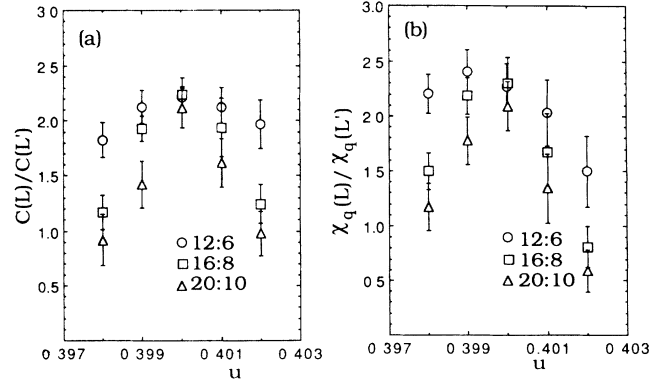


FIG. 2. (a) Ratio of specific heats $C(L)/C(L')$ and (b) ratio of charge-density susceptibilities $\chi_q(L)/\chi_q(L')$, plotted along a trajectory perpendicular to the phase boundary (see Fig. 1) passing through the point \mathcal{C} . Three different sets of lattice lengths $L:L'$ with equal ratio $\frac{1}{2}$ are shown. The common intersection of the three curves is at $(u_c, (L/L')^{2y_1 - d})$. Both C and χ_q show the same scaling behavior.

where $K \equiv 1/T$. From Eqs. (2) and (3), plots of $R_C(L, L') \equiv C(L)/C(L')$, along a trajectory in the u - T plane, for different L and L' , but the same ratio L/L' , should intersect only at the critical point¹³ \mathcal{C} , giving the value $R_C = (L/L')^{2y_1 - d}$. In Fig. 2(a) we plot $C(L)/C(L')$ for ratios 12:6, 16:8, and 20:10 as a function of u , computed along a trajectory passing through \mathcal{C} roughly perpendicular to the phase boundary. The three curves do indeed intersect at a single point $u_c = 0.4$, $T_c = 0.138$, with $R_C = 2.15 \pm 0.25$, giving $2y_1 - d = 1.10 \pm 0.16$. Since $d=2$, we have $y_1 \equiv 1/\nu = 1.55 \pm 0.08$.

Similarly, if u has a nonzero projection on g_1 , then the charge-density susceptibility,

$$\chi_q = \frac{1}{NT} \left[\left\langle \left(\sum_i q_i^2 \right)^2 \right\rangle - \left\langle \sum_i q_i^2 \right\rangle^2 \right] \\ = -T \frac{\partial^2 f}{\partial u^2} \sim L^{2y_1 - d}, \quad (4)$$

should have the same scaling behavior as the specific heat C . In Fig. 2(b) we plot $R_\chi(L, L') \equiv \chi_q(L)/\chi_q(L')$ along the same trajectory as before, for the same $L:L'$. Again all curves intersect at the same single point (u_c, T_c) , with $R_\chi = 2.2 \pm 0.3$ giving $y_1 = 1.57 \pm 0.10$.

Similarly, one can compute at the point \mathcal{C} the second derivative of f along any direction \hat{e} in the T - u plane, $f_{ee} \equiv (\hat{e} \cdot \nabla)^2 f(T_c, u_c)$,

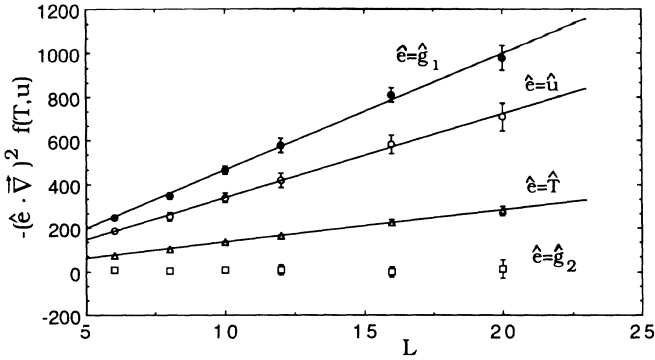


FIG. 3. Second derivative of the free energy $f(T, u)$, in the direction \hat{e} , evaluated at the critical point \mathcal{C} , as a function of lattice length L . For the T and u directions (corresponding to specific heat C and density susceptibility χ_q) we have the approximately linear scaling $L^{2y_1-d} \sim L$ (solid line is the best linear fit) found from Fig. 2. For direction g_2 tangent to the phase boundary, we have the scaling L^{2y_2-d} , with $y_2 < y_1$, corresponding to the second most relevant direction in the u - T phase space. The most relevant direction g_1 lies perpendicular to the phase boundary.

plot this directional second derivative of the free energy at the critical point \mathcal{C} , for directions $\hat{e} = \hat{g}_1, \hat{T}, \hat{u}$, and \hat{g}_2 , evaluated by computing the appropriate correlation functions (5). We find, as expected, that g_2 lies tangential to the phase boundary. g_1 is found to lie perpendicular to the phase boundary. For $\hat{e} = \hat{g}_1, \hat{T}$, and \hat{u} , we see the approximately linear scaling with L implicit in the results of Fig. 2. Along $\hat{e} = \hat{g}_2$, the scaling is consistent with a less divergent, sublinear behavior. The relatively large error bars along this direction, however, prevent a meaningful estimate of y_2 . The data shown in Figs. 2 and 3 represent Monte Carlo runs of 200 000 passes through the lattice, with an initial 10 000 passes discarded for equilibration. Error bars are estimated by block averaging.

To find the order-parameter exponent y_h , we have computed the square of the order parameter M^2 along the same trajectory as for C and χ_q above. As this trajectory is along the most relevant direction g_1 , we expect the scaling

$$M^2 = T \frac{\chi M}{L^d} = \frac{T^2}{L^d} \frac{\partial^2 f}{\partial h^2} = L^{2(y_h-d)} \Phi[(u-u_c)L^{y_1}]. \quad (6)$$

In Fig. 4 we show the results for lattice lengths from $L=6$ to 16. Here, runs of 800 000 passes were used for greater accuracy. The data for various L in Fig. 4 all appear to intersect at a single point, giving $d-y_h = \beta/\nu \approx 0$. We have fitted the scaling form (6) to a fourth-order expansion in $u-u_c$, using the procedure of Ref. 14. To test whether we have reached the large- L scaling limit, we drop data from successively lower values of L until the fitted parameters remain constant. In this way, using sizes from $L=10$ to 16, we find the best fit (solid

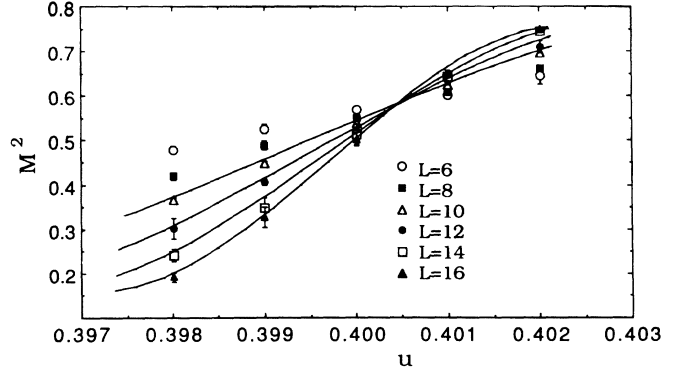


FIG. 4. Square of the Ising order parameter, $M^2 = (1/N) \sum_i q_i (-1)^{x_i+y_i}$, vs u along the same trajectory as for Fig. 2, for various lattice lengths L . The intersection of all the curves close to a common point indicates a scaling exponent $\beta \approx 0$. Solid lines are best fits to an expansion of the scaling function (6) using data from $L=10$ to 16.

lines in Fig. 4) to yield $d-y_h = 0.04 \pm 0.02$, $y_1 = 1.67 \pm 0.08$, and $u_c = 0.4 \pm 0.0003$, giving good agreement for y_1 and u_c as found in the analysis of C and χ_q .

As the Hamiltonian (1) has the symmetry of an anti-ferromagnetic Blume-Emery-Griffiths model,¹⁵ one might expect that the point \mathcal{C} is an Ising tricritical point. However, the exact exponents of the ordinary Ising tricritical point are¹² $y_1 = 1.8$, $d-y_h = 0.075$. If we compare the directly measured quantity $2y_1-d$, our finite-size scaling gives 1.10 ± 0.16 versus the Ising tricritical value of 1.6. We thus believe the point \mathcal{C} is not the usual Ising tricritical point, and perhaps reflects the effects of the long-range interaction between charge-density fluc-

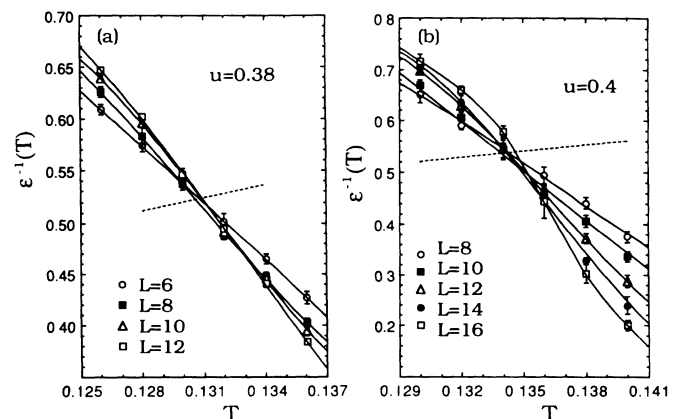


FIG. 5. Inverse dielectric function $\epsilon^{-1}(T)$ for constant (a) $u=0.38$ (just below first-order line) and (b) $u=0.4$ (just above first-order line) for various lattice sizes L . The common intersection of the curves for different L locates T_{KT} . Intersection with the dashed line $4T$ gives the Kosterlitz-Thouless prediction $\epsilon^{-1}(T_c^-) = 4T_{KT}$. Good agreement with this universal jump is found.

tuations.

Finally, the KT transitions (dashed lines) in Fig. 1 have been determined by calculating the inverse dielectric function,^{5,10,11}

$$\epsilon^{-1} = \lim_{k \rightarrow 0} 1 - \frac{2\pi}{Tk^2} \langle q_k q_{-k} \rangle, \quad q_k = \frac{1}{L} \sum_i e^{ik \cdot r_i} q_i, \quad (7)$$

which we evaluate at the smallest $k = 2\pi/L$ in a finite lattice. Since ϵ^{-1} maps onto the helicity modulus of the XY model,⁵ the Josephson scaling relation¹⁶ gives to leading order $\epsilon^{-1}(T, L) \sim L^{d-2} H[L/\xi(T)]$. As $d=2$, the intersection of the curves of different L locates T_{KT} . In Fig. 5 we plot $\epsilon^{-1}(T, L)$ at values $u=0.38$ just below the first-order line, and $u=0.4$ just above the first-order line. In both cases the value of T_{KT} given by scaling, lies very close to the KT prediction $\epsilon^{-1}(T_{KT}) = 4T_{KT}$, as determined by the intersection with the dashed line $4T$. We thus find no strong evidence¹⁷ for nonuniversal jumps in ϵ^{-1} . We note, however, that the KT lines are terminated by the first-order line at a temperature only slightly lower than the value $T^* \approx 0.14$ below which Minnhagen predicts nonuniversal behavior.⁷ Thus, deviation from the universal value, if it exists, might be too small for us to have detected.

We have benefited greatly by discussions with Professor P. Minnhagen, Professor E. Domany, Professor D. Mukamel, Professor K. K. Mon, and Dr. Y.-H. Li. This work has been supported by the Department of Energy under Grant No. DE-FG02-89ER14017.

¹For general reviews, see B. Nienhuis, in *Phase Transitions and Critical Phenomena*, edited by C. Domb and J. Lebowitz (Academic, London, 1987), Vol. 11, p. 1; P. Minnhagen, *Rev. Mod. Phys.* **59**, 1001 (1987).

²J. V. José, L. P. Kadanoff, S. Kirkpatrick, and D. R. Nel-

son, *Phys. Rev. B* **16**, 1217 (1977).

³B. I. Halperin and D. R. Nelson, *J. Low Temp. Phys.* **36**, 599 (1979); V. Ambegaokar, B. I. Halperin, D. R. Nelson, and E. D. Siggia, *Phys. Rev. B* **21**, 1806 (1980).

⁴J. M. Kosterlitz and D. Thouless, *J. Phys. C* **6**, 1181 (1973); J. M. Kosterlitz, *J. Phys. C* **7**, 1046 (1974).

⁵D. R. Nelson and J. M. Kosterlitz, *Phys. Rev. Lett.* **39**, 1201 (1977); T. Ohta and D. Jasnow, *Phys. Rev. B* **20**, 130 (1979); P. Minnhagen and G. G. Warren, *Phys. Rev. B* **24**, 2526 (1981).

⁶R. H. Swendsen, *Phys. Rev. Lett.* **49**, 1302 (1982); E. Domany, M. Schick, and R. H. Swendsen, *Phys. Rev. Lett.* **52**, 1535 (1984); J. E. Van Himbergen, *Phys. Rev. Lett.* **53**, 5 (1984); *Phys. Rev. B* **29**, 6387 (1984).

⁷P. Minnhagen, *Phys. Rev. Lett.* **54**, 2351 (1985); *Phys. Rev. B* **32**, 3088 (1985).

⁸J. M. Thijssen and H. J. F. Knops, *Phys. Rev. B* **38**, 9080 (1988); P. Minnhagen and M. Wallin, *Phys. Rev. B* **40**, 5109 (1989).

⁹S. Teitel and C. Jayaprakash, *Phys. Rev. B* **27**, 598 (1983); *Phys. Rev. Lett.* **51**, 1999 (1983).

¹⁰J. M. Thijssen and H. J. F. Knops, *Phys. Rev. B* **37**, 7738 (1988).

¹¹G. S. Grest, *Phys. Rev. B* **39**, 9267 (1989).

¹²For a review, see I. D. Lawrie and S. Sarbach, in *Phase Transitions and Critical Phenomena*, edited by C. Domb and J. Lebowitz (Academic, London, 1984), Vol. 9, p. 1.

¹³M. N. Barber and W. Selke, *J. Phys. A* **15**, L617 (1982).

¹⁴Y.-H. Li and S. Teitel, *Phys. Rev. B* **40**, 9122 (1989).

¹⁵M. Blume, V. J. Emery, and R. B. Griffiths, *Phys. Rev. A* **4**, 1071 (1971).

¹⁶B. D. Josephson, *Phys. Lett.* **21**, 608 (1966); M. E. Fisher, M. N. Barber, and D. Jasnow, *Phys. Rev. A* **8**, 1111 (1973).

¹⁷A more careful attempt at finite-size scaling, including leading logarithmic corrections in the prefactor of the scaling function $H(L/\xi)$, is given in H. Weber and P. Minnhagen, *Phys. Rev. B* **37**, 5986 (1988). We have tried to fit our data as described there. Our results were consistent with the universal jump, but our numerical accuracy could not rule out a $\sim 5\%$ deviation.